



An Observer-Based Topology Identification and Synchronization in Finite Time for Fractional Singularly Perturbed Complex Networks via Dynamic Event-Triggered Control

Lingyan Wang¹ · Huaiqin Wu¹ · Jinde Cao^{2,3}

Accepted: 8 May 2024
© The Author(s) 2024

Abstract

This paper investigates the topology identification and synchronization in finite time for fractional singularly perturbed complex networks (FSPCNs). Firstly, a convergence principle is developed for continuously differential functions. Secondly, a dynamic event-triggered mechanism (DETM) is designed to achieve the network synchronization, and a topology observer is developed to identify the network topology. Thirdly, under the designed DETM, by constructing a Lyapunov functional and applying the inequality analysis technique, the topology identification and synchronization condition in finite time is established in the forms of the matrix inequality. In addition, it is proved that the Zeno behavior can be effectively excluded. Finally, the effectiveness of the main results is verified by an application example.

Keywords Fractional complex networks · Event-triggered mechanism · Synchronization · Topology identification

1 Introduction

Complex dynamical networks (CDNs), which contains a large amount of nodes with the communication topology, are ubiquitous in nature and human society, such as transportation networks, biological networks, power networks and so on [1–4]. Generally, the dynamics of CDNs are determined by the topology structure and dynamical properties of nodes, which indicates that the dynamical behavior of CDNs is difficult to understand when the communication topology is unknown [5–7]. Hence, it is significant to identify the topology of CDNs, see [8–19] and references therein.

✉ Huaiqin Wu
huaiqinwu@ysu.edu.cn
Jinde Cao
jdcao@seu.edu.cn

¹ School of Science, Yanshan University, Qinhuangdao 066001, China

² School of Mathematics, Southeast University, Nanjing 210096, China

³ Ahlia University, Manama 10878, Bahrain

Recently, a plenty of studies are concentrated on the topology identification of CDNs, and some results are achieved. For example, in [11], Zhu et al. researched the topology identification of CDNs via synchronization method and an auxiliary network, which composed of isolated nodes. In [12], a novel method was developed to solve topology identification for Hindmarsh-Rose neural networks with sinusoidal signals when the persistently excite conditions could not hold. In [13], the topology identification for CDNs with multiple links was considered by utilizing adaptive control method and building chaotic auxiliary networks.

Since the fractional calculus can describe the various processes with memory and hereditary characteristics more accurately than integral calculus, see [20, 21], CDNs described by fractional calculus received wide attention from scholars. More recently, many works have been put into topology identification for fractional complex dynamical networks (FCDNs) [15–19]. Particularly, in [18], the topology identification was discussed for FCDNs via inequality techniques and synchronization-based method. In [19], Bai et al. considered the secure synchronization and topology identification for FCDNs under Denial of Service (DoS) attacks by using feedback control method.

It should be pointed out that, in the control mechanism in [14–19], the feedback / adaptive controller is used to deal with the synchronization of CDNs. Nevertheless, the adaptive/ feedback control mechanism requires to update data continuously, which will lead to additional information communication and waste of resources. To address the drawback, the event-triggered control (ETC) determined by static rule is proposed, and some results about the synchronization of CDNs were obtained by applying static ETC. see [22–26]. In static ETC, information is updated only when the threshold is less than or equal to the measurement error.

In order to mitigate the communication burden more effectively, in recent works, the dynamic event-triggered control (DETC) mechanism is presented, where a dynamic variable was added to the event-triggered condition. For example, in [29], Li et al. considered the synchronization for variable-order fractional piecewise-smooth networks by DETC, and established the exponential synchronization criterion. The mean-square exponential synchronization in a stochastic complex network was investigated via intermittent DETC in [30].

It is worth noting that in the aforementioned results, for CDNs, the time-scale characteristics of all nodes are required to be the same. However, in real world, 'fast' dynamics and 'slow' dynamics may coexist in one system, which can be modeled as a singularly perturbation system, such as circuit systems, high-speed aircraft systems, etc. [31–34]. Recently, SPCNs have attracted considerable concern of many scholars [35–44]. Particularly, in [37], Rakkiyappan et al. explored the state estimation and synchronization for SPCNs by sampling control method. In [39], the stochastic synchronization was studied for SPCNs with impulsive effects and semi-markov jump topology. It should be pointed out that, in the aforementioned papers about SPCNs [36–44], the topology structure of the CNs is set to be known. As far as we know, few results are focused on the topology identification for FSPCNs. Hence, the main motivation of this paper is to design topology observer and control strategy with DETM, derive synchronization and identification conditions for FSPCNs.

Inspired by the above discussion, the objective of this article is to tackle the problems of the topology identification and synchronization for FSPCNs. In this paper, the main contributions are listed below.

- 1) In the existing results [15] and [18], the topology identification and synchronization are considered for FCDNs. The topology identification and synchronization are considered for fractional CDNs with the singularly perturbation in this work. Compared with [15] and [18], the results in this paper are more universal.

Table 1 Notation

Symbols	Meanings
N, C	Integer, complex numbers set
N^+	Positive integer numbers set
R	Real numbers set
R^n	n -dimensional real vector set
$R^{n \times m}$	$n \times m$ real matrices set
$ x $	Absolute value of x
$\ x\ $	$= (\sum_{i=1}^n x_i ^2)^{\frac{1}{2}}$
I_M	M -dimensional identify matrix
$\text{diag}(a, b, \dots, c)$	Diagonal matrix
$C^n[a, b]$	n -order continuously differentiable Function
\otimes	Kronecker product of two matrices
$\lambda_{\min}(A) (\lambda_{\max}(A))$	the minimum(maximum) Eigenvalue of A
A^{-1} / A^T	Inverse/Transpose of matrix A
$A > 0$	$A \in R^{n \times n}$, and is positive definite

- 2) An topology observer and a DETM are designed to realize the topology identification and synchronization for FSPCNs. Compared with the control methods used in [23, 25], the control strategy adopted in this paper can save resource more efficiently.
- 3) The finite-time synchronization condition is established based on a novel ε -dependent Lyapunov function, by the matrix inequality. In addition, the topology identification is successfully realized.

The remainders of this paper are arranged as follows. In section 2, some important lemmas, definitions and properties are introduced. The system description is provided in Sect. 3. In Sect. 4, the main results of the topology identification and synchronization for FSPCNs are discussed. In section 5, an application example is presented to verify the correctness of the theoretical results. Section 6 gives some conclusions.

Notation: See Table 1.

2 Preliminaries

Definition 1 ([20]) For $f(\tau) \in C^n[t_0, +\infty)$. Caputo fractional derivative of α -order is defined as

$${}_t^c D_{t_0}^\alpha f(\tau) = \frac{1}{\Gamma(n - \alpha)} \int_{t_0}^\tau \frac{f^{(n)}(v)}{(\tau - v)^{1+n-\alpha}} dv,$$

where $\tau \geq t_0$, $\Gamma(\cdot)$ is Gamma function, $\alpha \in (n - 1, n)$, $n \in N$. Especially, if $\alpha \in (0, 1)$,

$${}_t^c D_{t_0}^\alpha f(\tau) = \frac{1}{\Gamma(1-\alpha)} \int_{t_0}^\tau \frac{f'(v)}{(\tau-v)^\alpha} dv.$$

Definition 2 ([20]) For $f(\tau) : [t_0, +\infty) \rightarrow R$, Riemann-Liouville fractional integral of α -order is defined as

$${}_t^R I_{t_0}^\alpha f(\tau) = \frac{1}{\Gamma(\alpha)} \int_{t_0}^\tau \frac{f(v)}{(\tau - v)^{1-\alpha}} dv,$$

where $\alpha > 0$, and $\Gamma(\alpha) = \int_0^\infty e^{-t} t^{\alpha-1} dt$.

For convenience, I^α and D^α are used to denote ${}_t^c I_{t_0}^\alpha$ and ${}_t^c D_{t_0}^\alpha$ in the following.

Property 1. ([20]). Properties of fractional derivatives

- (i) when $\alpha \geq \beta > 0$, $D^\alpha I^\beta f(\tau) = D^{\alpha-\beta} f(\tau)$;
Especially, $D^\alpha I^\beta f(\tau) = f(\tau)$, where $\alpha = \beta$, $0 < \alpha \leq 1$.
- (ii) $D^\alpha u = 0$, where u is a constant.
- (iii) $D^\alpha (u_1 f(\tau) + u_2 g(\tau)) = u_1 D^\alpha f(\tau) + u_2 D^\alpha g(\tau)$,
where u_1, u_2 are constants.
- (iv) If $f(\tau) \in C^n([t_0, +\infty), R)$, then $I^\alpha D^\alpha f(\tau) = f(\tau) - \sum_{k=0}^{n-1} \frac{f^{(k)}(t_0)}{k!} (\tau - t_0)^k$.
Especially, if $0 < \alpha \leq 1$ and $0 < t < T$, then $D^\alpha I^\alpha f(\tau) = f(\tau)$, $I^\alpha D^\alpha f(\tau) = f(\tau) - f(t_0)$.

Definition 3 ([21]). Mittag-Leffler function $E_{\dot{\alpha}, \ddot{\alpha}}(\tau)$ is defined as

$$E_{\dot{\alpha}, \ddot{\alpha}}(\tau) = \sum_{k=1}^\infty \frac{\tau^k}{\Gamma(k\dot{\alpha} + \ddot{\alpha})},$$

where $\tau \in C$, $\dot{\alpha} > 0$, $\ddot{\alpha} > 0$. When $\ddot{\alpha} = 1$,

$$E_{\dot{\alpha}, 1}(\tau) = E_{\dot{\alpha}}(\tau) = \sum_{k=1}^\infty \frac{\tau^k}{\Gamma(k\dot{\alpha} + 1)}.$$

In particular, when $\ddot{\alpha} = 1$, $\dot{\alpha} = 1$, $E_{1,1}(\tau) = e^\tau$.

Lemma 1 ([19]). Let $0 < \alpha \leq 1$. $G \in R^{n \times n}$, and $G > 0$. Suppose that $r(\tau) \in R^n$ is a function, which is continuously differentiable. Then,

$$D^\alpha (r^T(\tau) G r(\tau)) \leq 2r^T(\tau) G D^\alpha r(\tau)$$

holds, for any $\tau \geq t_0$.

Lemma 2 ([38]). Let $\varepsilon \in (0, \varepsilon']$, $0 < \varepsilon' \leq 1$. If there exist symmetric matrices Q_1, Q_3 , and matrix Q_2 , such that $\begin{pmatrix} Q_1 & \varepsilon' Q_2^T \\ \varepsilon' Q_2 & Q_3 \end{pmatrix} > 0$, $Q_1 > 0$, then $E(\varepsilon) Q(\varepsilon) = Q^T(\varepsilon) E(\varepsilon) > 0$,

where $Q(\varepsilon) = \begin{pmatrix} Q_1 & \varepsilon Q_2^T \\ Q_2 & Q_3 \end{pmatrix}$.

Lemma 3 ([38]). Let $\check{\alpha} \in (0, 1)$. If $\mathcal{V}(\tau)$ is continuously differentiable on $[t_0, +\infty)$, and satisfies

$$D^{\check{\alpha}} \mathcal{V}(\tau) \leq -v \mathcal{V}(\tau), \quad \tau \geq t_0,$$

where v is a positive constant, then,

$$\mathcal{V}(\tau) \leq \mathcal{V}(t_0) E_{\check{\alpha}}(-v(\tau - t_0)^{\check{\alpha}}), \quad \tau \geq t_0.$$

Lemma 4 ([38]). *Let ω is a positive constant. $z_i \in R^n, i = 1, 2$. The following inequality*

$$z_1^T z_2 \leq \frac{\omega}{2} z_1^T z_1 + \frac{1}{2\omega} z_2^T z_2,$$

holds.

Lemma 5 *If there is a positive definite function $\mathcal{V}(\tau) \in C^1([t_0, +\infty), R), \check{\alpha} \in (0, 1)$ such that*

$$D^{\check{\alpha}} \mathcal{V}(\tau) \leq -\zeta \mathcal{V}(\tau) - \mu, \tag{1}$$

where $\zeta > 0$, and $\mu > 0$. Then, $\lim_{\tau \rightarrow T} \mathcal{V}(\tau) = 0$, and $\mathcal{V}(\tau) \equiv 0$, for $\tau \geq T$. T is the solution of the equation

$$p E_{\check{\alpha}}(-\zeta(\tau - t_0)^{\check{\alpha}}) - \frac{\mu}{\zeta} = 0,$$

where $p = \frac{\mu}{\zeta} + \mathcal{V}(t_0)$.

Proof Applying Property 1, from (1), it follows that,

$$D^{\check{\alpha}}(\mathcal{V}(\tau) + \frac{\mu}{\zeta}) \leq -\zeta(\mathcal{V}(\tau) + \frac{\mu}{\zeta}).$$

Set $\mathcal{V}(\tau) + \frac{\mu}{\zeta} = \tilde{\mathcal{V}}(\tau)$,

$$D^{\check{\alpha}} \tilde{\mathcal{V}}(\tau) \leq -\zeta \tilde{\mathcal{V}}(\tau).$$

According to Lemma 3, we have

$$\tilde{\mathcal{V}}(\tau) \leq \tilde{\mathcal{V}}(t_0) E_{\check{\alpha}}(-\zeta(\tau - t_0)^{\check{\alpha}}).$$

The above inequality can be represented as

$$\mathcal{V}(\tau) \leq (\mathcal{V}(t_0) + \frac{\mu}{\zeta}) E_{\check{\alpha}}(-\zeta(\tau - t_0)^{\check{\alpha}}) - \frac{\mu}{\zeta}.$$

Since $E_{\check{\alpha}}(-\zeta(\tau - t_0)^{\check{\alpha}})$ is monotonically decreasing function, there exists $T > t_0$, such that $(\mathcal{V}(t_0) + \frac{\mu}{\zeta}) E_{\check{\alpha}}(-\zeta(T - t_0)^{\check{\alpha}}) - \frac{\mu}{\zeta} = 0$, and $\mathcal{V}(\tau) \leq 0$, for $\tau \geq T$. Noting that $\mathcal{V}(\tau) \geq 0$, for $\tau \geq 0$, this derives that $\mathcal{V}(\tau) \equiv 0, \tau \geq T$. This completes the proof. \square

3 Description of Network Model

Consider a nonlinear FSPCNs with M identical nodes described by singularly perturbation system

$$\begin{aligned} E(\varepsilon) D^\alpha x_i(t) &= \begin{bmatrix} D^\alpha x_{1i}(t) \\ \varepsilon D^\alpha x_{2i}(t) \end{bmatrix} \\ &= f(x_i(t)) + d \sum_{j=1}^M b_{ij} \Gamma x_j(t), \end{aligned} \tag{2}$$

where $\alpha \in (0, 1), t \in [t_0, +\infty), \varepsilon$ is the perturbation parameter satisfying $0 < \varepsilon \leq \varepsilon' \ll 1$; $E(\varepsilon) = \begin{bmatrix} I_{n_1} & 0 \\ 0 & \varepsilon I_{n_2} \end{bmatrix}; x_i(t) = \begin{bmatrix} x_{1i}(t) \\ x_{2i}(t) \end{bmatrix} \in R^{n_1+n_2}$ is state vector of i -th node at time

$t, i = 1, 2, \dots, M$, where $x_{1i}(t) = (x_{1i1}(t), x_{1i2}(t), \dots, x_{1in_1}(t))^T \in R^{n_1}$, $x_{2i}(t) = (x_{2i1}(t), x_{2i2}(t), \dots, x_{2in_2}(t))^T \in R^{n_2}$; The nonlinear function $f(x_i(t)) = \begin{bmatrix} f^1(x_{1i}(t)) \\ f^2(x_{2i}(t)) \end{bmatrix} \in R^{n_1+n_2}$, where $f^1(x_{1i}(t)) = (f_1^1(x_{1i1}(t)), f_2^1(x_{1i2}(t)), \dots, f_{n_1}^1(x_{1in_1}(t)))^T \in R^{n_1}$, $f^2(x_{2i}(t)) = (f_1^2(x_{2i1}(t)), f_2^2(x_{2i2}(t)), \dots, f_{n_2}^2(x_{2in_2}(t)))^T \in R^{n_2}$; d represents the coupling strength; $\Gamma = \text{diag}(\varrho_1, \varrho_2, \dots, \varrho_{n_1+n_2}) \in R^{(n_1+n_2) \times (n_1+n_2)}$ is internal coupling matrix; $B = [b_{ij}]_{M \times M}$ denotes an unknown weight construction matrix, which stands for the topology in network (2). If there is a connection between nodes j and i ($j \neq i$), then $b_{ij} \neq 0$, if not, $b_{ij} = 0$ ($j \neq i$). In addition, $b_{ii} = -\sum_{j=1, j \neq i}^M b_{ij}$.

In the following, for network (2), we design a response network described by

$$\begin{aligned}
 E(\varepsilon)D^\alpha y_i(t) &= \begin{bmatrix} D^\alpha y_{1i}(t) \\ \varepsilon D^\alpha y_{2i}(t) \end{bmatrix} \\
 &= f(y_i(t)) + d \sum_{j=1}^M \hat{b}_{ij}(t)\Gamma y_j(t) + u_i(t),
 \end{aligned}
 \tag{3}$$

where $y_i(t) = \begin{bmatrix} y_{1i}(t) \\ y_{2i}(t) \end{bmatrix}$ is state vector of y -th node at time $t, i = 1, 2, \dots, M$, in which $y_{1i}(t) = (y_{1i1}(t), y_{1i2}(t), \dots, y_{1in_1}(t))^T \in R^{n_1}$, $y_{2i}(t) = (y_{2i1}(t), y_{2i2}(t), \dots, y_{2in_2}(t))^T \in R^{n_2}$; The function $f(y_i(t)) = \begin{bmatrix} f^1(y_{1i}(t)) \\ f^2(y_{2i}(t)) \end{bmatrix} \in R^{n_1+n_2}$, where $f^1(y_{1i}(t)) = (f_1^1(y_{1i1}(t)), f_1^1(y_{1i2}(t)), \dots, f_{n_1}^1(y_{1in_1}(t)))^T \in R^{n_1}$, $f^2(y_{2i}(t)) = (f_1^2(y_{2i1}(t)), f_2^2(y_{2i2}(t)), \dots, f_{n_2}^2(y_{2in_2}(t)))^T \in R^{n_2}$. $\hat{B}(t) = [\hat{b}_{ij}(t)]_{M \times M}$ is a known weight construction matrix, which is used to identify unknown matrix B ; $u_i(t)$ is the control input. The other parameters are the same as in (2).

In order to obtain the main results of this article, the following assumptions are made for $f(\cdot)$ and unknown weight b_{ij} :

(\mathcal{H}_1): For $f_i(\cdot), s_1 \neq s_2$, the following condition is satisfied

$$0 \leq \frac{f_i(s_1) - f_i(s_2)}{s_1 - s_2} \leq z_i,$$

where z_i is a positive constant.

(\mathcal{H}_2): For weight b_{ij} , which is norm bounded, such that

$$|b_{ij}| \leq M_b, i, j = 1, 2, \dots, M,$$

where $M_b > 0$ is a constant.

The synchronization error for the i -th node is represented by $e_i(t)$, and $e_i(t) = y_i(t) - x_i(t)$. Together (2) with (3), the synchronization error system can be expressed as

$$\begin{aligned}
 E(\varepsilon)D^\alpha e_i(t) &= \check{f}(e_i(t)) + d \sum_{j=1}^M \tilde{b}_{ij}(t)\Gamma y_j(t) \\
 &+ d \sum_{j=1}^M b_{ij}\Gamma e_j(t) + u_i(t),
 \end{aligned}
 \tag{4}$$

where $\tilde{b}_{ij}(t) = \hat{b}_{ij}(t) - b_{ij}$, $\check{f}(e_i(t)) = f(y_i(t)) - f(x_i(t)), i, j = 1, 2, \dots, M$.

Definition 4 Let $x_i(t)$ be the solutions of (2) with initial value $x_i(t_0) = x_{i0}$, $y_i(t)$ be the solutions of (3) with initial value $y_i(t_0) = y_{i0}$.

1). If there exist $T(e_i(t_0)) \geq t_0$, satisfy

$$\lim_{t \rightarrow T(e_i(t_0))} \|e_i(t)\| = 0, \text{ and } e_i(t) \equiv 0, \quad t \geq T(e_i(t_0)),$$

then system (2) and (3) are deemed to achieve synchronization in $T(e_i(t_0))$ under the controller $u(t)$. In addition, $T(e_i(t_0))$ is called as setting time.

2). If $\lim_{t \rightarrow T(e_i(t_0))} \tilde{b}_{ij}(t) = 0, \quad j, i = 1, 2, \dots, M$, then the topology in network (2) is said to realize the identification in finite time $T(e_i(t_0))$.

4 Main Result

In this paper, our focus is to establish the conditions that ensure the synchronization of networks (2) and (3), and to identify the topology in network (2) based on DETC. To do so, the controller $u_i(t)$ is designed as

$$u_i(t) = -K e_i(t_k^i) - c \frac{e_i(t_k^i) \text{sgn}(e_i(t_k^i))}{\|e_i(t_k^i)\|^2}, \quad t \in [t_k^i, t_{k+1}^i), \tag{5}$$

where c is positive constant; $\text{sgn}(\cdot)$ denotes signum function; K is the control gain matrix to be designed. $\{t_k^i\}$ denotes event-triggered sequence that satisfies $0 \leq t_0^i < t_1^i < t_2^i < \dots < t_k^i < \dots, k \in N^+$ and $\lim_{t \rightarrow \infty} t_k^i = +\infty$.

Remark 1 The signum function, as a simple nonlinear function, can be easily applied in controller (5) $u(t)$ compare to any other functions. During the operation of the controller, there is no need for complex mathematical calculations and function approximation, which helps to reduce the computational load of controller updates. Furthermore, in the proof in Theorem 1, the signum function term $e_i(t_k^i) \text{sgn}(e_i(t_k^i))$ plays a crucial role in eliminating the terms $\vartheta_i e_i^T(t_k^i) e_i(t_k^i)$ and $\bar{e}_i^T(t) \bar{e}_i(t)$.

Define the measurement error $\bar{e}_i(t)$ as $\bar{e}_i(t) = (y_i(t_k^i) - x_i(t_k^i)) - (y_i(t) - x_i(t)) = e_i(t_k^i) - e_i(t)$.

Design DETM as

$$t_{k+1}^i = \inf_{t > t_k^i} \left\{ t : \bar{e}_i^T(t) \bar{e}_i(t) \geq \vartheta_i e_i^T(t_k^i) e_i(t_k^i) + \gamma_i \eta_i(t) \right\}, \tag{6}$$

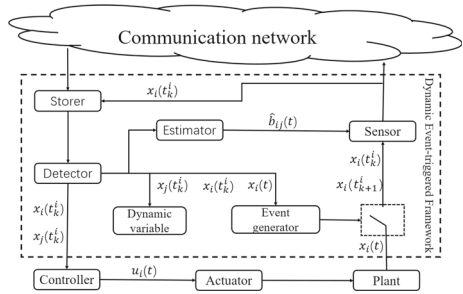
where ϑ_i, γ_i are positive constants, and $0 < \vartheta_i < 1; \eta_i(t)$ expresses an internal dynamic variable, and designed by

$$D^\alpha \eta_i(t) = -\beta_i \eta_i(t) - \frac{1}{2} c \frac{\gamma_i \eta_i(t)}{\|e_i(t_k^i)\|^2} + \vartheta_i e_i^T(t_k^i) e_i(t_k^i) - \bar{e}_i^T(t) \bar{e}_i(t), \tag{7}$$

where parameter $\beta_i > 0$. The framework of DETM (6) is depicted in Fig. 1.

Remark 2 1) In DETM (6), internal dynamic variable $\eta_i(t)$ is introduced, such that the threshold function $\vartheta_i e_i^T(t_k^i) e_i(t_k^i) + \gamma_i \eta_i(t)$ is adjustable. Due to $\eta_i(t) > 0$, the average interval

Fig. 1 Framework of DETC scheme



time can be enlarged, and the frequency of events triggered can be reduced effectively and Zeno behavior can be avoided.

2) In [27], DETM was designed as $t_{k+1}^i = \inf_{t > t_k^i} \{t : \bar{e}_i^T(t)\bar{e}_i(t) \geq \vartheta_i e_i^T(t)e_i(t) + \gamma_i \eta_i(t)\}$. Since the threshold function contains a continuous term $\vartheta_i e_i^T(t)e_i(t)$, the state information is requested to be known at all time. However, in practical application, not all of state information is available, which may cause the above event-triggering mechanism to be unavailable.

In [28], DETM was designed as $t_{k+1} = \inf_{t > t_k} \{t : \bar{e}_i^T(t)\bar{e}_i(t) \geq \gamma_i \eta_i(t) + \beta_i e^{-\alpha t} + \delta\}$, $\beta_i, \delta > 0$. Obviously, the threshold function is independent of system states, which may cause that the control law cannot update in time.

The designed DETM (6) is only required to know the state information at time t_k^i , and instead of all. It is easy to see that, controller updates depend on both internal dynamic variable $\eta_i(t)$ and state information $\bar{e}_i^T(t_k^i)$ at time t_k^i . Compared with [27] and [28], the designed DETM (6) is more superiority.

Remark 3 ETC updates the controller only when the certain triggering condition (6) is met, rather than updating the controller at fixed time intervals. Applying ETC to deal with FSPCNs synchronization can reduce the demand for communication resources, and improves the overall efficiency of the system operation.

To achieve the purpose of the topology identification for network (2) via controller (5) with DETM (6), we design the update law of the topology observer $\hat{b}_{ij}(t)$ as

$$D^\alpha \hat{b}_{ij}(t) = -\rho \text{sgn}(\tilde{b}_{ij}(t))(|\hat{b}_{ij}(t)| + M_b) - d \xi_{ij} e_i^T(t) Q^T(\varepsilon) \Gamma y_j(t). \tag{8}$$

where $\rho > 0$, and $\xi_{ij} > 0$ are real parameter to be designed.

Substitute (5) into (4), for $t \in [t_k^i, t_{k+1}^i)$, yields

$$E(\varepsilon) D^\alpha e_i(t) = \check{f}(e_i(t)) + d \sum_{j=1}^M b_{ij} \Gamma e_j(t) + d \sum_{j=1}^M \tilde{b}_{ij}(t) \Gamma y_j(t) - K e_i(t_k^i) - c \frac{e_i(t_k^i) \text{sgn}(e_i(t_k^i))}{\|e_i(t_k^i)\|^2}. \tag{9}$$

Lemma 6 Consider the designed DETM in (6) with (7). If $\eta_i(t_0^i) > 0$, then, $\eta_i(t) > 0, t \geq t_0^i, i = 1, 2, \dots, M$.

Proof For $t \in [t_k^i, t_{k+1}^i)$, applying (6) yields

$$\bar{e}_i^T(t) \bar{e}_i(t) \leq \vartheta_i e_i^T(t_k^i) e_i(t_k^i) + \gamma_i \eta_i(t). \tag{10}$$

By (10) and (7), it follows that

$$D^\alpha \eta_i(t) \geq -\beta_i \eta_i(t) - \gamma_i \eta_i(t) = -\pi_i \eta_i(t), \tag{11}$$

where $\pi_i = \beta_i + \gamma_i$.

On the basis of Lemma 3, from (11), we get

$$\eta_i(t) \geq \eta_i(t_k^i) E_\alpha(-\pi_i(t - t_k^i)^\alpha), \quad t \in [t_k^i, t_{k+1}^i).$$

$k \in \{0\} \cup N^+$.

Hence, for $t \in [t_0^i, t_{k+1}^i)$, we obtain that

$$\eta_i(t) \geq \eta_i(t_0^i) \left(\prod_{r=1}^k E_\alpha(-\pi_i(t_r^i - t_{r-1}^i)^\alpha) \right) E_\alpha(-\pi_i(t - t_k^i)^\alpha).$$

According to Definition 3 and $\eta_i(t_0^i) > 0$, from the above inequality, it can be derived that $\eta_i(t) \geq 0$, for $t \geq t_0$. The proof is completed.

If the dynamic variable $\eta_i(t) \equiv 0$, then DETM (6) changes to a static ETM in [27].

4.1 Synchronization and Topology Identification of FSPCNs

In this subsection, the synchronization and topology identification in finite time are realized between network (2) and (3) under controller (5) and observer (8).

Theorem 1 Let $\alpha \in (0, 1)$, and $\varepsilon \in (0, \varepsilon')$. Under the assumptions (\mathcal{H}_1) - (\mathcal{H}_2) , if there exist scalar $\omega > 0$, matrix $Q_1 > 0$, matrix Q_2 and symmetric matrix Q_3 , such that

$$(i) \begin{pmatrix} Q_1 & \varepsilon' Q_2^T \\ \varepsilon' Q_3 \end{pmatrix} > 0;$$

$$(ii) \frac{1}{2} I_M \otimes (Q^T(\varepsilon) Q(\varepsilon)) + d(B \otimes Q^T(\varepsilon) \Gamma) + \frac{\omega}{2} I_M \otimes (Q^T(\varepsilon) K K^T Q(\varepsilon)) - \frac{1}{2} I_M \otimes (Q^T(\varepsilon) K + K^T Q(\varepsilon)) \leq -\frac{\varepsilon}{2} I_{M(n_1+n_2)},$$

hold, then system (2) and (3) can achieve the finite-time synchronization under controller (5). The setting time $T(e_i(t_0))$ is the solution of equality

$$\left(\mathcal{V}(t_0) + \frac{\mu_i}{\zeta_i} \right) E_\alpha \left(-\zeta_i(t - t_0)^\alpha \right) - \frac{\mu_i}{\zeta_i} = 0,$$

where $\zeta_i = \min \left\{ \frac{2}{\lambda_{\max}(Q(\varepsilon)E(\varepsilon))} (\lambda_{\min}(\Theta)), 2\rho, \beta_i + \gamma_i \right\}$, $\Theta = -\frac{\varepsilon}{2} I_{M(n_1+n_2)} - \frac{1}{2} I_M \otimes (Q^T(\varepsilon) Q(\varepsilon)) - d(B \otimes Q^T(\varepsilon) \Gamma) - \frac{\omega}{2} I_M \otimes (Q^T(\varepsilon) K K^T Q(\varepsilon)) + \frac{1}{2} I_M \otimes (Q^T(\varepsilon) K + K^T Q(\varepsilon))$,

$$\mu_i = \frac{1}{2} c \lambda_{\min}(Q^T(\varepsilon)) (1 - \vartheta_i),$$

$$\mathcal{V}(t_0) = \frac{1}{2} \sum_{i=1}^M (y_{i0} - x_{i0})^T E(\varepsilon) Q(\varepsilon) (y_{i0} - x_{i0}) + \sum_{i=1}^M \eta_i(t_0) + \frac{1}{2} \sum_{i=1}^M \sum_{j=1}^M \frac{1}{\xi_{ij}} (\hat{b}_{ij}(t_0) - b_{ij})^2.$$

In addition, the topology of system (2) can be identified in finite time under update law of the topology observer (8) successfully.

Proof Consider the following Lyapunov function:

$$\mathcal{V}(t) = \mathcal{V}_1(t) + \mathcal{V}_2(t) + \mathcal{V}_3(t), \tag{12}$$

where $\mathcal{V}_1(t) = \frac{1}{2} \sum_{i=1}^M e_i^T(t) E(\varepsilon) Q(\varepsilon) e_i(t)$, $\mathcal{V}_2(t) = \sum_{i=1}^M \eta_i(t)$, and $\mathcal{V}_3(t) = \frac{1}{2} \sum_{i=1}^M \sum_{j=1}^M \frac{1}{\xi_{ij}} (\hat{b}_{ij}(t) - b_{ij})^2$.

For $t \in [t_k^i, t_{k+1}^i)$, according to Lemmas 1 and 4, calculating Caputo fractional derivative of α -order for $\mathcal{V}_1(t)$ along with the solution of system (9), yields

$$\begin{aligned}
 D^\alpha \mathcal{V}_1(t) &\leq \sum_{i=1}^M e_i^T(t) Q^T(\varepsilon) E(\varepsilon) D^\alpha e_i(t) \\
 &= \sum_{i=1}^M e_i^T(t) Q^T(\varepsilon) \check{f}(e_i(t)) \\
 &\quad + d \sum_{i=1}^M \sum_{j=1}^M b_{ij} e_i^T(t) Q^T(\varepsilon) \Gamma e_j(t) \\
 &\quad + d \sum_{i=1}^M \sum_{j=1}^M \tilde{b}_{ij}(t) e_i^T(t) Q^T(\varepsilon) \Gamma y_j(t) \\
 &\quad - \sum_{i=1}^M e_i^T(t) Q^T(\varepsilon) K e_i(t_k^i) \\
 &\quad - c \frac{|e_i^T(t_k^i) - \bar{e}_i^T(t)| Q^T(\varepsilon) e_i(t_k^i)}{\|e_i(t_k^i)\|^2} \\
 &\leq \sum_{i=1}^M e_i^T(t) \left(\frac{1}{2} Q^T(\varepsilon) Q(\varepsilon) - Q^T(\varepsilon) K \right. \\
 &\quad \left. d \sum_{j=1}^M b_{ij} Q^T(\varepsilon) \Gamma + \frac{\omega}{2} Q^T(\varepsilon) K K^T Q(\varepsilon) \right) e_i(t) \\
 &\quad + d \sum_{i=1}^M \sum_{j=1}^M \tilde{b}_{ij}(t) e_i^T(t) Q^T(\varepsilon) \Gamma y_j(t) \\
 &\quad + \frac{1}{2} \sum_{i=1}^M \check{f}^T(e_i(t)) \check{f}(e_i(t)) - \sum_{i=1}^M \frac{1}{2\omega} \bar{e}_i^T(t) \bar{e}_i(t) \\
 &\quad + c \frac{\lambda_{\min}(Q^T(\varepsilon)) (-\|e_i^T(t_k^i)\|^2 + |\bar{e}_i^T(t)| e_i(t_k^i))}{\|e_i(t_k^i)\|^2}.
 \end{aligned} \tag{13}$$

For $t \in [t_k^i, t_{k+1}^i)$, by computing Caputo fractional derivative of α -order of $\mathcal{V}_2(t)$ along with the solution of system (7), one obtains

$$\begin{aligned}
 D^\alpha \mathcal{V}_2(t) &= \sum_{i=1}^M D^\alpha \eta_i(t) = \sum_{i=1}^M (-\beta_i \eta_i(t)) \\
 &\quad - \frac{1}{2} c \frac{\gamma_i \eta_i(t)}{\|e_i(t_k^i)\|^2} + \vartheta_i e_i^T(t_k^i) e_i(t_k^i) - \bar{e}_i^T(t) \bar{e}_i(t).
 \end{aligned} \tag{14}$$

For $t \in [t_k^i, t_{k+1}^i)$, calculating Caputo fractional derivative of α -order of $\mathcal{V}_3(t)$ along with the solution of system (8), it yields

$$\begin{aligned}
 D^\alpha \mathcal{V}_3(t) &= \sum_{i=1}^M \sum_{j=1}^M \frac{1}{\xi_{ij}} (\hat{b}_{ij}(t) - b_{ij}) D^\alpha \hat{b}_{ij}(t) \\
 &= -\rho \sum_{i=1}^M \sum_{j=1}^M \frac{1}{\xi_{ij}} \tilde{b}_{ij}(t) \operatorname{sgn}(\tilde{b}_{ij}(t)) (|\hat{b}_{ij}(t)| + M_b) \\
 &\quad - d \sum_{i=1}^M \sum_{j=1}^M \tilde{b}_{ij}(t) e_i^T(t) Q^T(\varepsilon) \Gamma y_j(t).
 \end{aligned} \tag{15}$$

From (\mathcal{H}_2) , it can be obtained that $|\hat{b}_{ij}(t)| + M_b \geq |\hat{b}_{ij}(t) - b_{ij}| = |\tilde{b}_{ij}(t)|$. Hence,

$$\begin{aligned}
 &-\rho \sum_{i=1}^M \sum_{j=1}^M \frac{1}{\xi_{ij}} \tilde{b}_{ij}(t) (\operatorname{sgn}(\tilde{b}_{ij}(t)) (|\hat{b}_{ij}(t)| + M_b)) \\
 &\leq -\rho \sum_{i=1}^M \sum_{j=1}^M \frac{1}{\xi_{ij}} (\tilde{b}_{ij}(t))^2.
 \end{aligned} \tag{16}$$

On the basis of (12)-(16), for $t \in [t_k^i, t_{k+1}^i)$, one has

$$\begin{aligned}
 D^\alpha \mathcal{V}(t) &\leq \sum_{i=1}^M e_i^T(t) \left(\frac{1}{2} Q^T(\varepsilon) Q(\varepsilon) - Q^T(\varepsilon) K \right. \\
 &\quad \left. + d \sum_{j=1}^M b_{ij} Q^T(\varepsilon) \Gamma + \frac{\omega}{2} Q^T(\varepsilon) K K^T Q(\varepsilon) \right) e_i(t) \\
 &\quad - \sum_{i=1}^M \frac{1}{2\omega} \bar{e}_i^T(t) \bar{e}_i(t) - \rho \sum_{i=1}^M \sum_{j=1}^M \frac{1}{\xi_{ij}} (\tilde{b}_{ij}(t))^2 \\
 &\quad - \sum_{i=1}^M \bar{e}_i^T(t) \bar{e}_i(t) + \sum_{i=1}^M \vartheta_i e_i^T(t_k^i) e_i(t_k^i) \\
 &\quad + \frac{1}{2} \sum_{i=1}^M \check{f}^T(e_i(t)) \check{f}(e_i(t)) - \sum_{i=1}^M \beta_i \eta_i(t) \\
 &\quad + c \frac{\lambda_{\min}(Q^T(\varepsilon)) (-\|e_i^T(t_k^i)\|^2 + |\bar{e}_i^T(t)| e_i(t_k^i))}{\|e_i(t_k^i)\|^2}.
 \end{aligned} \tag{17}$$

Due to (\mathcal{H}_1) , we have $\check{f}^T(e_i(t)) \check{f}(e_i(t)) \leq z e_i^T(t) e_i(t)$, where $z = \max_{1 \leq i \leq M} \{z_i^2\}$.

Utilizing Property 1 and DETM (6), it follows from (17) that,

$$\begin{aligned}
 D^\alpha \mathcal{V}(t) &\leq \sum_{i=1}^M e_i^T(t) \left(\frac{1}{2} Q^T(\varepsilon) Q(\varepsilon) - Q^T(\varepsilon) K \right. \\
 &\quad + \frac{\omega}{2} Q^T(\varepsilon) K K^T Q(\varepsilon) + d \sum_{j=1}^M b_{ij} Q^T(\varepsilon) \Gamma \\
 &\quad \left. + \frac{z}{2} I_{M(n_1+n_2)} \right) e_i(t) - \rho \sum_{i=1}^M \sum_{j=1}^M \frac{1}{\xi_{ij}} (\tilde{b}_{ij}(t))^2 \\
 &\quad - \sum_{i=1}^M \left(\beta_i + \frac{1}{2} c \frac{\gamma_i \eta_i(t)}{\|e_i(t_k^i)\|^2} + \gamma_i \right) \eta_i(t) \\
 &\quad + c \frac{\lambda_{\min}(Q^T(\varepsilon)) (\frac{1}{2} \bar{e}_i^T(t) \bar{e}_i(t) - \frac{1}{2} \|e_i^T(t_k^i)\|^2)}{\|e_i(t_k^i)\|^2} \\
 &\leq e^T(t) \left(\frac{1}{2} I_M \otimes (Q^T(\varepsilon) Q(\varepsilon)) + d(B \otimes Q^T(\varepsilon) \Gamma) \right. \\
 &\quad + \frac{\omega}{2} I_M \otimes (Q^T(\varepsilon) K K^T Q(\varepsilon)) - \frac{1}{2} I_M \otimes (Q^T(\varepsilon) K \\
 &\quad + K^T Q(\varepsilon)) + \frac{z}{2} I_{M(n_1+n_2)} \left. \right) e(t) - \sum_{i=1}^M (\beta_i \\
 &\quad + \frac{1}{2} c \frac{\gamma_i \eta_i(t)}{\|e_i(t_k^i)\|^2} + \gamma_i) \eta_i(t) - \rho \sum_{i=1}^M \sum_{j=1}^M \frac{1}{\xi_{ij}} (\tilde{b}_{ij}(t))^2 \\
 &\quad - \frac{1}{2} c \lambda_{\min} Q^T(\varepsilon) \left(1 - \frac{\|\bar{e}(t)\|^2}{\|e(t_k)\|^2} \right) \\
 &\leq e^T(t) \left(\frac{1}{2} I_M \otimes (Q^T(\varepsilon) Q(\varepsilon)) + d(B \otimes Q^T(\varepsilon) \Gamma) \right. \\
 &\quad + \frac{\omega}{2} I_M \otimes (Q^T(\varepsilon) K K^T Q(\varepsilon)) - \frac{1}{2} I_M \otimes (Q^T(\varepsilon) K \\
 &\quad + K^T Q(\varepsilon)) + \frac{z}{2} I_{M(n_1+n_2)} \left. \right) e(t) \\
 &\quad - \sum_{i=1}^M (\beta_i + \gamma_i) \eta_i(t) - \rho \sum_{i=1}^M \sum_{j=1}^M \frac{1}{\xi_{ij}} (\tilde{b}_{ij}(t))^2 \\
 &\quad - \frac{1}{2} c \lambda_{\min}(Q^T(\varepsilon)) (1 - \vartheta_i) \leq -\zeta_i \mathcal{V}(t) - \mu_i,
 \end{aligned} \tag{18}$$

where $\zeta_i = \min\{\frac{2}{\lambda_{\max}(Q(\varepsilon)E(\varepsilon))} (\lambda_{\min}(\Theta)), 2\rho, \beta_i + \gamma_i\}$, $\Theta = -\frac{z}{2} I_{M(n_1+n_2)} - \frac{1}{2} I_M \otimes (Q^T(\varepsilon) Q(\varepsilon)) - d(B \otimes Q^T(\varepsilon) \Gamma) - \frac{\omega}{2} I_M \otimes (Q^T(\varepsilon) K K^T Q(\varepsilon)) + \frac{1}{2} I_M \otimes (Q^T(\varepsilon) K + K^T Q(\varepsilon))$; $\mu_i = \frac{1}{2} c \lambda_{\min}(Q^T(\varepsilon)) (1 - \vartheta_i)$.

By Lemma 5, we can conclude that $\lim_{t \rightarrow T(e_i(t_0))} \mathcal{V}(t) = 0$, and $\mathcal{V}(t) \equiv 0$, for $t \geq T(e_i(t_0))$,

where $T(e_i(t_0))$ is the solution of equality $\left(\mathcal{V}(t_0) + \frac{\mu_i}{\zeta_i} \right) E_\alpha \left(-\zeta_i (t - t_0)^\alpha \right) - \frac{\mu_i}{\zeta_i} = 0$.

Moreover, from the expression of $\mathcal{V}(t)$, it can be obtained that, $\lim_{t \rightarrow T(e_i(t_0))} \|e_i(t)\| = \lim_{t \rightarrow T(e_i(t_0))} \tilde{b}_{ij}(t) = 0$, and $\|e_i(t)\| = \tilde{b}_{ij}(t) \equiv 0$, for $t \geq T(e_i(t_0))$. This shows that, system (2) and (3) can achieve the synchronization in finite time under observer (8) and controller (5), and the unknown topology in network (2) can be identified in finite time. The proof is complete.

Remark 4 In [15], the topology identification and synchronization were considered for fractional CDNs by the adaptive feedback control strategy. In [44], the synchronization was studied for SPCNs by the DETC method, but the topology identification issue was not discussed.

In Theorem 1, the synchronization and topology identification in finite time are exploited for FSPCNs concurrently on the basis of DETC. Obviously, the results of this paper are an improvement and extension for that in [15] and [44].

Remark 5 In the proof of Theorem 1, an ε -dependent Lyapunov function is introduced by incorporating the parameter ε into the traditional Lyapunov function for system stability analysis. The introduction of ε can enhance the sensitivity of the Lyapunov function, and then respond to smaller changes in the system state, and has stronger analytical ability than the traditional Lyapunov function. Moreover, if the parameter $\varepsilon = 1$, the ε -dependent Lyapunov function becomes a general Lyapunov function, hence, the range of applications of the ε -dependent Lyapunov function is wider.

In Theorem 1, we have investigated $\varepsilon \in (0, 1)$ in FSPCNs (2) and (3). In the following Case 1) and 2), we discuss the synchronization and topology identification in finite time between networks (2) and (3) when $\varepsilon = 0$ and $\varepsilon = 1$, respectively.

Case 1). Systems (2) and (3) become as

$$\begin{aligned} E(0)D^\alpha x_i(t) &= \begin{pmatrix} D^\alpha x_{1i}(t) \\ 0 \end{pmatrix} \\ &= f(x_i(t)) + d \sum_{j=1}^M b_{ij} \Gamma x_j(t), \end{aligned} \tag{19}$$

$$\begin{aligned} E(0)D^\alpha y_i(t) &= \begin{pmatrix} D^\alpha y_{1i}(t) \\ 0 \end{pmatrix} \\ &= f(y_i(t)) + d \sum_{j=1}^M \hat{b}_{ij}(t) \Gamma y_j(t) + u_i(t), \end{aligned} \tag{20}$$

respectively, where $E(0) = \begin{bmatrix} I_{n_1} & 0 \\ 0 & 0 \end{bmatrix}$.

Corollary 1 Let $\alpha \in (0, 1)$. Under the assumptions (\mathcal{H}_1) - (\mathcal{H}_2) , if there exist scalar $\omega > 0$, matrix Q_2 and positive definite matrices Q_1, Q_3 , such that

- (i) $E(0)Q(0) \geq 0$.
- (ii) $\frac{1}{2}I_M \otimes (Q^T(0)Q(0)) + d(B \otimes Q^T(0)\Gamma) + \frac{\omega}{2}I_M \otimes (Q^T(0)KK^TQ(0)) - \frac{1}{2}I_M \otimes (Q^T(0)K + K^TQ(0)) \leq -\frac{\zeta}{2}I_{M(n_1+n_2)}$, hold, where $Q(0) = \begin{pmatrix} Q_1 & 0 \\ Q_2 & Q_3 \end{pmatrix}$, then system (19) and (20) can achieve the finite time synchronization under controller (5). The setting time $T(e_i(t_0))$ is the solution of equality

$$\left(\mathcal{V}(t_0) + \frac{\mu_i}{\zeta_i}\right) E_\alpha\left(-\zeta_i(t-t_0)^\alpha\right) - \frac{\mu_i}{\zeta_i} = 0,$$

where $\zeta_i = \min \left\{ \frac{2}{\lambda_{\max}(Q(0)E(0))} (\lambda_{\min}(\Theta)), 2\rho, \beta_i + \gamma_i \right\}$, $\Theta = -\frac{\zeta}{2} I_{M(n_1+n_2)} - \frac{1}{2} I_M \otimes (Q^T(0)Q(0)) - d(B \otimes Q^T(0)\Gamma) - \frac{\omega}{2} I_M \otimes (Q^T(0)K K^T Q(0)) + \frac{1}{2} I_M \otimes (Q^T(0)K + K^T Q(0))$, $\mu_i = \frac{1}{2} c \lambda_{\min}(Q^T(0))(1 - \vartheta_i)$, $\mathcal{V}(t_0) = \frac{1}{2} \sum_{i=1}^M (y_{i0} - x_{i0})^T E(0) Q(0) (y_{i0} - x_{i0}) + \sum_{i=1}^M \eta_i(t_0) + \frac{1}{2} \sum_{i=1}^M \sum_{j=1}^M \frac{1}{\xi_{ij}} (\hat{b}_{ij}(t_0) - b_{ij})^2$.

In addition, the topology of system (19) can be identified in finite time under update law of the topology observer (8) successfully.

Case 2). Systems (2) and (3) change as

$$D^\alpha x_i(t) = f(x_i(t)) + d \sum_{j=1}^M b_{ij} \Gamma x_j(t), \tag{21}$$

$$D^\alpha y_i(t) = f(y_i(t)) + d \sum_{j=1}^M \hat{b}_{ij}(t) \Gamma y_j(t) + u_i(t), \tag{22}$$

respectively.

Corollary 2 Let $\alpha \in (0, 1)$. Under the assumptions (\mathcal{H}_1) - (\mathcal{H}_2) , if there exist scalar $\omega > 0$, matrix $Q > 0$, such that

$$\begin{aligned} & \frac{1}{2} I_M \otimes (Q^T Q) + d(B \otimes Q^T \Gamma) + \frac{\omega}{2} I_M \otimes (Q^T K K^T Q) \\ & - \frac{1}{2} I_M \otimes (Q^T K + K^T Q) \leq -\frac{\zeta}{2} I_{M(n_1+n_2)}, \end{aligned}$$

hold, then system (21) and (22) can achieve the finite-time synchronization under controller (5). The setting time $T(e_i(t_0))$ is the solution of equality

$$\left(\mathcal{V}(t_0) + \frac{\mu_i}{\zeta_i} \right) E_\alpha \left(-\zeta_i(t - t_0)^\alpha \right) - \frac{\mu_i}{\zeta_i} = 0,$$

where $\zeta_i = \min \left\{ \frac{2}{\lambda_{\max}(Q)} (\lambda_{\min}(\Theta)), 2\rho, \beta_i + \gamma_i \right\}$, $\Theta = -\frac{1}{2} I_M \otimes (Q^T Q) - d(B \otimes Q^T \Gamma) - \frac{\omega}{2} I_M \otimes (Q^T K K^T Q) + \frac{1}{2} I_M \otimes (Q^T K + K^T Q) - \frac{\zeta}{2} I_{M(n_1+n_2)}$, $\mu_i = \frac{1}{2} c \lambda_{\min}(Q)(1 - \vartheta_i)$, $\mathcal{V}(t_0) = \frac{1}{2} \sum_{i=1}^M (y_{i0} - x_{i0})^T Q (y_{i0} - x_{i0}) + \sum_{i=1}^M \eta_i(t_0) + \frac{1}{2} \sum_{i=1}^M \sum_{j=1}^M \frac{1}{\xi_{ij}} (\hat{b}_{ij}(t_0) - b_{ij})^2$.

In addition, the topology of system (21) can be identified in finite time under the update law of the topology observer (8) successfully.

Remark 6 When set $\varepsilon = 0$, system (19) and (20) become fractional singular CDNs, which means that network nodes are connected only in slow dynamical mode, the fast dynamical connection do not exist. When take $\varepsilon = 1$, networks (21) and (22) change as fractional CDNs without the singular perturbation, and there is only a fast dynamic connection mode between networks. Corollary 1 and 2 discuss the synchronization and topology identification of FSPCNs in the above two cases respectively.

Remark 7 Traditional synchronization methods, such as asymptotic synchronization and exponential synchronization [17, 18], generally require an infinite time for a system to achieve

synchronization. Finite-time synchronization method achieves the estimability of the synchronization time. Designers can adjust control parameters based on the estimated time to meet specific synchronization requirements.

4.2 Exclusion of Zeno Phenomenon

For the designed event-triggering mechanism (6), in the following, it is proved that the Zeno behavior can be excluded.

Theorem 2 *For each node, under the designed event-triggering mechanism (6), the Zeno phenomenon will not occur.*

Proof From the proof process of Theorem 1, we can conclude that, there exists a positive constant \bar{h} , such that $\|Q^T(\varepsilon)E(\varepsilon)D^\alpha e_i(t)\| \leq \bar{h}, i = 1, 2, \dots, M$. Noting that $\bar{e}_i(t) = e_i(t_k^i) - e_i(t)$, we have $\bar{e}_i(t_k^i) = 0$. It derives that, $E(\varepsilon)D^\alpha \bar{e}_i(t) = -E(\varepsilon)D^\alpha e_i(t)$. Hence,

$$\begin{aligned} \|\bar{e}_i(t)\| &= \|e_i(t_k^i) - e_i(t)\| \\ &= \|E^{-1}(\varepsilon)Q^{-T}(\varepsilon)D^{-\alpha}D^\alpha Q^T(\varepsilon)E(\varepsilon)(e_i(t_k^i) - e_i(t))\| \\ &= \|E^{-1}(\varepsilon)Q^{-T}(\varepsilon)\frac{1}{\Gamma(\alpha)}\int_{t_k^i}^t(t-s)^{\alpha-1}D^\alpha Q^T(\varepsilon)E(\varepsilon)\bar{e}_i(s)ds\| \\ &= \|E^{-1}(\varepsilon)Q^{-T}(\varepsilon)\frac{1}{\Gamma(\alpha)}\int_{t_k^i}^t(t-s)^{\alpha-1}Q^T(\varepsilon)E(\varepsilon)D^\alpha e_i(s)ds\| \tag{23} \\ &\leq \|E^{-1}(\varepsilon)Q^{-T}(\varepsilon)\|\frac{1}{\Gamma(\alpha)}\int_{t_k^i}^t(t-s)^{\alpha-1}\|Q^T(\varepsilon)E(\varepsilon)D^\alpha e_i(s)\|ds \\ &\leq \frac{\bar{h}\|E^{-1}(\varepsilon)Q^{-T}(\varepsilon)\|(t-t_k^i)^\alpha}{\Gamma(\alpha+1)}. \end{aligned}$$

For $t \in [t_k^i, t_{k+1}^i)$, under the event-triggering mechanism (6), it yields

$$\|\bar{e}_i(t)\| \geq (\gamma_i \eta_i(t) + \vartheta_i e_i^T(t_k^i)e_i(t_k^i))^{\frac{1}{2}}. \tag{24}$$

Let $\Delta = t_{k+1}^i - t_k^i$. Together (23) with (24), it follows that,

$$(\gamma_i \eta_i(t_{k+1}^i) + \vartheta_i e_i^T(t_k^i)e_i(t_k^i))^{\frac{1}{2}} \leq \frac{\bar{h}\|E^{-1}(\varepsilon)Q(\varepsilon)\|\Delta^\alpha}{\Gamma(\alpha+1)}.$$

By means of Lemma 6, we can obtain that

$$\Delta \geq \left(\frac{\Gamma(\alpha+1)(\gamma_i \eta_i(t_{k+1}^i) + \vartheta_i \|e_i(t_k^i)\|^2)^{\frac{1}{2}}}{\bar{h}\|E^{-1}(\varepsilon)Q(\varepsilon)\|} \right)^{\frac{1}{\alpha}} > 0.$$

This means that, under the designed event-triggering mechanism(6), the Zeno phenomenon will not occur. □

5 A Simulation Example

Here, a simulation example is provided to demonstrate the correctness of the theoretical results of this paper.

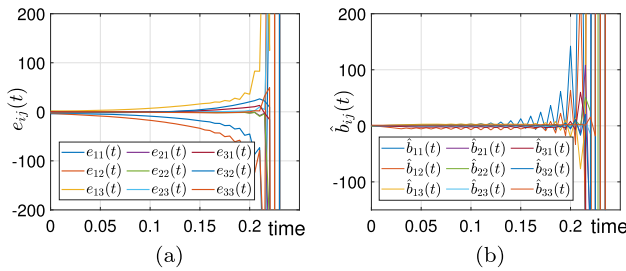


Fig. 2 The curves of $e_{ij}(t)$ and $\hat{b}_{ij}(t)$ without controller

Consider a 3-dimensional FSPCNs with 3 nodes, where the dynamic of nodes is described by Lorenz system:

$$E(\varepsilon)D^\alpha x_i(t) = f(x_i(t)) + d \sum_{j=1}^3 b_{ij}\Gamma x_j(t), \tag{25}$$

where $i, j = 1, 2, 3; d = 0.02; \varepsilon = 0.27, \varepsilon' = 0.3; B = (b_{ij})_{3 \times 3}$ and Γ are chosen as

$$B = \begin{bmatrix} 2.4 & -5.2 & 2.8 \\ 0 & 1.0 & -1.0 \\ -2.3 & 0.4 & 1.9 \end{bmatrix}, \quad \Gamma = \begin{bmatrix} 1.52 & 0 & 0 \\ 0 & 0.351 & 0 \\ 0 & 0 & 3.105 \end{bmatrix}.$$

$$f(x_i(t)) = \begin{bmatrix} -10 & 10 & 0 \\ 28 & -1 & 0 \\ 0 & 0 & -8/3 \end{bmatrix} \begin{bmatrix} x_{i1}(t) \\ x_{i2}(t) \\ x_{i3}(t) \end{bmatrix} + \begin{bmatrix} 0 \\ -x_{i1}(t)x_{i3}(t) \\ x_{i1}(t)x_{i2}(t) \end{bmatrix}.$$

Network (25) is considered as the drive network, the corresponding response network is

$$E(\varepsilon)D^\alpha y_i(t) = f(y_i(t)) + d \sum_{j=1}^3 \hat{b}_{ij}(t)\Gamma y_j(t) + u_i(t), \tag{26}$$

where the parameters α, d, Γ are same as that in the drive network (25). In addition, the update law of the observer $\hat{b}_{ij}(t)$ is described by

$$D^\alpha \hat{b}_{ij}(t) = -\rho \text{sgn}(\tilde{b}_{ij}(t))(|\hat{b}_{ij}(t)| + 5.2) - d\xi_{ij}e_i^T(t)Q^T(\varepsilon)\Gamma y_j(t)$$

where $\rho = 0.1; \xi_{ij} = 1, i, j = 1, 2, 3; Q_1 = \begin{bmatrix} 1.3105 & 0.061 \\ 0.061 & 1.7092 \end{bmatrix}, Q_2 = [0.68 \ 0.566], Q_3 = [5.433], d$ and Γ are same as that in (25).

1). When $u_i(t) = 0$, the trajectories of the error $e_{ij}(t)$ and topology observer $\hat{b}_{ij}(t)$ are depicted in Fig. 2 (a) and (b), respectively. It is easy to see that, network (25) and (26) can not achieve the synchronization, and the topology of network (25) can not also be identified in finite time.

2). For DETM (6) with (7), set $c = 1.004$, other parameters are shown in Table 2. For system (7), take initial values $\eta_1(0) = 1.8, \eta_2(0) = 2.7, \eta_3(0) = 2.0$ of the internal dynamic variable $\eta(t)$.

Let $t_0 = 0$. Take the initial values $x_1(0) = (-1.320, -2.140, 1.035)^T, x_2(0) = (-3.070, -1.852, -2.041)^T, x_3(0) = (-1.331, 2.508, -0.901)^T$ for network (25), and

Table 2 Parameter values in (6) with (7)

ϑ	Value	γ	Value	β	Value
ϑ_1	0.954	γ_1	0.018	β_1	0.047
ϑ_2	0.681	γ_2	0.216	β_2	0.004
ϑ_3	0.332	γ_3	0.012	β_3	0.019

Fig. 3 Chaotic attractor of Lorenz system with $\alpha = 0.97$

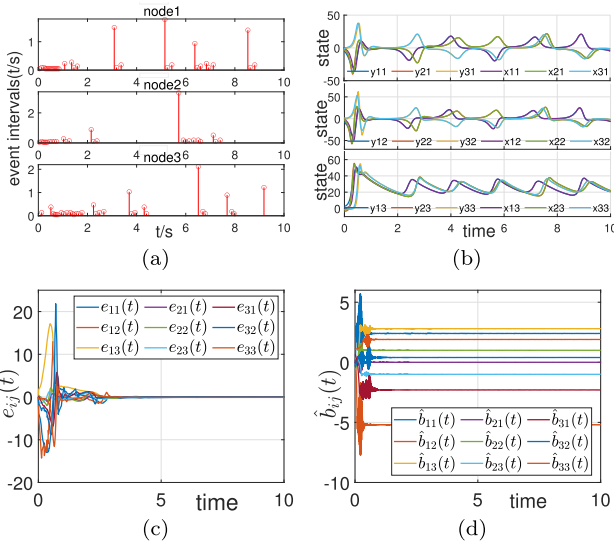
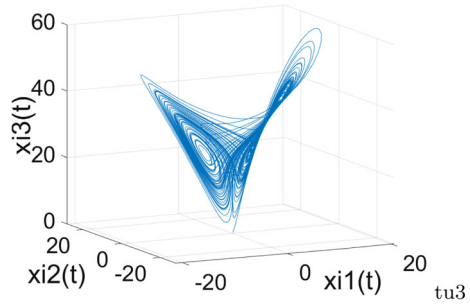


Fig. 4 In 2) ① $\alpha = 0.97$: **a** The event intervals based on DETM (6); **b** The trajectories of $x_{ij}(t)$ and $y_{ij}(t)$; **c** The trajectories of $e_{ij}(t)$; **d** The trajectories of $\hat{b}_{ij}(t)$; $i, j = 1, 2, 3$

$y_1(0) = (-5.330, -5.503, 2.761)^T$, $y_2(0) = (-3.791, -1.030, -3.547)^T$, $y_3(0) = (-0.842, 0.571, -1.415)^T$ for network (26). Under above parameters, the system states at three different orders are plotted in Figs. 3, 4, 5, 6, 7 and 8.

①. Fractional order $\alpha = 0.97$. The Chaotic attractor of Lorenz system is shown in Fig. 3. By solving the inequality (ii) in Theorem 1, the control gain K in the controller (5) can be calculated as

$$K = \begin{bmatrix} 2.71 & 2.10 & 4.25 \\ -0.14 & -14.12 & -7.06 \\ 1.40 & -4.61 & -7.51 \end{bmatrix}.$$

Fig. 5 Chaotic attractor of Lorenz system with $\alpha = 0.8$

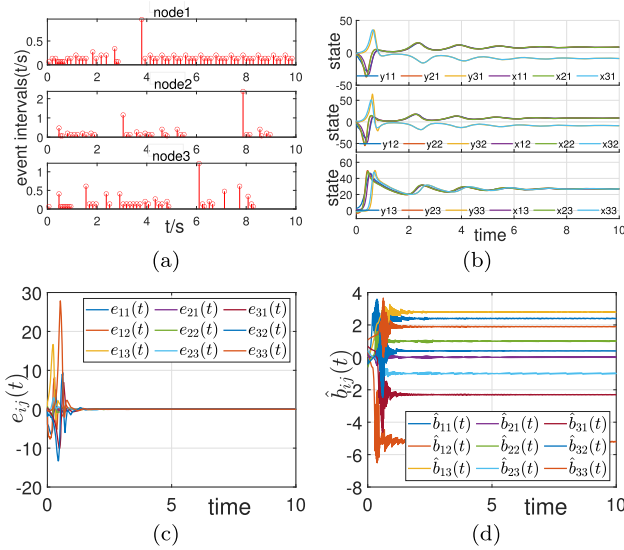
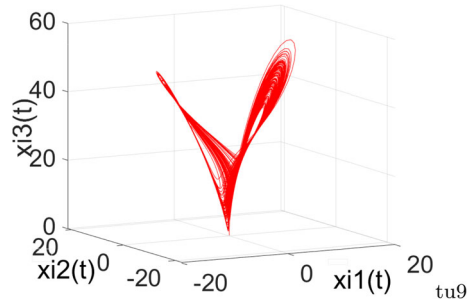
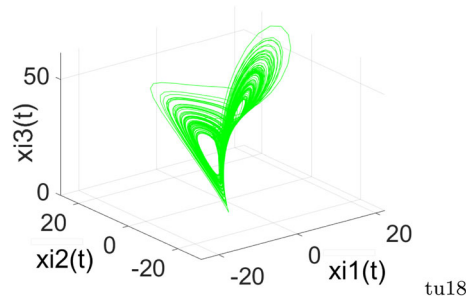


Fig. 6 In 2) $\alpha = 0.8$: **a** The event intervals based on DETM (6); **b** The trajectories of $x_{ij}(t)$ and $y_{ij}(t)$; **c** The trajectories of $e_{ij}(t)$; **d** The trajectories of $\hat{b}_{ij}(t)$; $i, j = 1, 2, 3$

Fig. 7 Chaotic attractor of Lorenz system with $\alpha = 0.7$



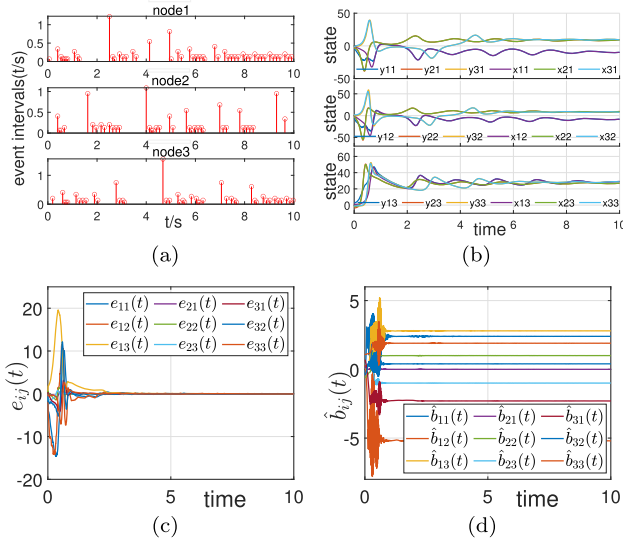


Fig. 8 In 2) ③ $\alpha = 0.7$: **a** The event intervals based on DETM (6); **b** The trajectories of $x_{ij}(t)$ and $y_{ij}(t)$; **c** The trajectories of $e_{ij}(t)$; **d** The trajectories of $\hat{b}_{ij}(t)$; $i, j = 1, 2, 3$

And, on the basis of Theorem 1, the setting time $T(e_i(t_0))$ is calculated as $T(e_i(t_0)) = 4.7041$. The corresponding simulation results are depicted in Fig. 4.

②. Fractional order $\alpha = 0.8$. The Chaotic attractor of Lorenz system is displayed in Fig. 5. The control gain K can be computed as

$$K = \begin{bmatrix} -0.43 & 3.27 & 1.20 \\ -1.65 & -5.72 & -8.24 \\ 2.25 & -3.28 & 2.12 \end{bmatrix}.$$

The setting time $T(e_i(t_0))$ is calculated as $T(e_i(t_0)) = 3.3156$ based Theorem 1. The corresponding simulation results are shown in Fig. 6.

③. Fractional order $\alpha = 0.7$. Figure 7 shows the corresponding Chaotic attractor of Lorenz system. By solving the inequality (ii) in Theorem 1, the control gain K in the controller (5) can be derived as

$$K = \begin{bmatrix} 4.13 & 3.55 & 1.95 \\ -0.07 & -8.14 & -4.68 \\ 3.07 & -1.77 & -2.58 \end{bmatrix}.$$

The setting time $T(e_i(t_0))$ is calculated as $T(e_i(t_0)) = 5.258$. The corresponding simulation results are displayed in Fig. 8.

From Figs. 3, 4, 5, 6, 7 and 8, we can see that, in the cases of three different values of fractional order α , the synchronization error $e_{ij}(t)$ converges to zero in finite, which indicates that the systems (25) and (26) can achieve the finite-time synchronization, and the topology in network (25) is identified successfully.

3). In [25], the event-triggering mechanism is designed as

$$t_{k+1}^i = \inf_{t > t_k^i} \{t : \bar{e}_i^T(t) \bar{e}_i(t) \geq \vartheta_i e_i^T(t_k^i) e_i(t_k^i) + e^{-\varsigma t}\}.$$

Take fractional order $\alpha = 0.97$, and simulate system (25) and (26) under controller in [25] and the above parameters. The results are depicted in Fig. 9. In addition, the corresponding

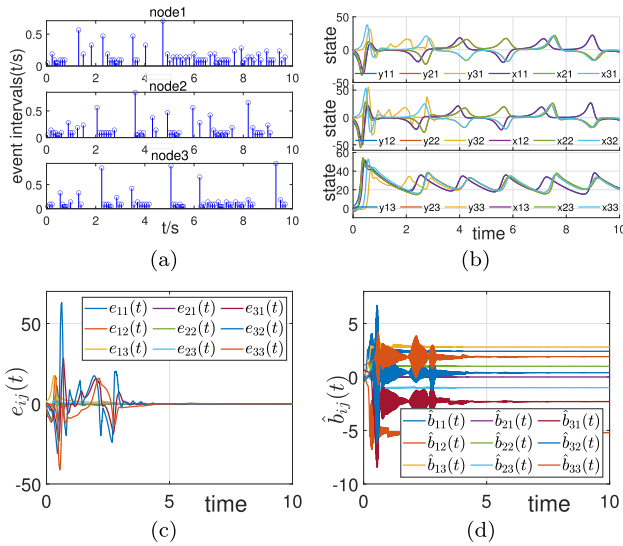


Fig. 9 $\alpha = 0.97$: **a** The event intervals based on DETM [25]; **b** The trajectories of $x_{ij}(t)$ and $y_{ij}(t)$; **c** The trajectories of $e_{ij}(t)$; **d** The trajectories of $\hat{b}_{ij}(t)$; $i, j = 1, 2, 3$

Table 3 Event-triggering times and intervals in [25] and the example

Node	[25]				This example			
	Triggering times	Min. interval	Max. interval	Ave. interval	Triggering times	Min. interval	Max. interval	Ave. interval
1	66	0.049	0.782	0.093	36	0.062	1.782	0.149
2	58	0.067	0.952	0.210	28	0.187	3.329	0.541
3	68	0.271	1.429	0.425	33	0.405	2.011	0.407

event-triggered intervals and times by using the control mechanism in [25] and the control mechanism in this example, which are recorded in Table 2. Compared with [25], in this example, the event-triggering times are reduced obviously, and the event-triggered interval is magnified. This indicates that the designed DETM (6) can save communication resources more effectively than the event-triggering mechanism in [25] and has better control effect (Table 3).

4). Taking $\alpha = 0.97$, based on the above parameters, we verify the results of Corollary 1 and 2. The corresponding results are shown in Figs. 10 and 11. Figure 10 shows the system trajectory with $\varepsilon = 0$, and Fig. 11 shows the system trajectory with $\varepsilon = 1$.

From Figs. 10 and 11, it can be seen that, the synchronization error $e_{ij}(t)$ converges to zero in finite time. This implies that $\varepsilon = 0$ and $\varepsilon = 1$, the systems (25) and (26) can achieve the finite-time synchronization. On the basis of Corollary 1, the setting time $T(e_i(t_0))$ is calculated as $T(e_i(t_0)) = 4.6913$, and from Corollary 2, it can be get $T(e_i(t_0)) = 6.4287$. In addition, the identification trajectories of $\hat{b}_{ij}(t)$ is depicted in Figs. 10d and 11d. From Figs. 10d and 11d, we conclude that the topology in network (25) is identified successfully.

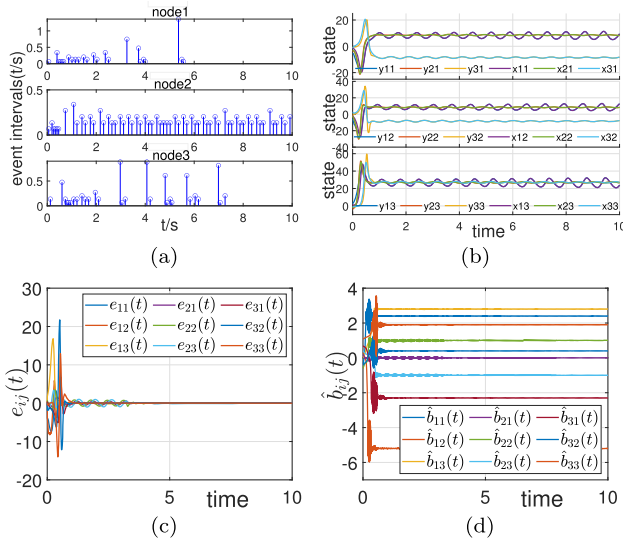


Fig. 10 Corollary 1 $\alpha = 0.7$: **a** The event intervals based on DETM (6); **b** The trajectories of $x_{ij}(t)$ and $y_{ij}(t)$; **c** The trajectories of $e_{ij}(t)$; **d** The trajectories of $\hat{b}_{ij}(t)$; $i, j = 1, 2, 3$

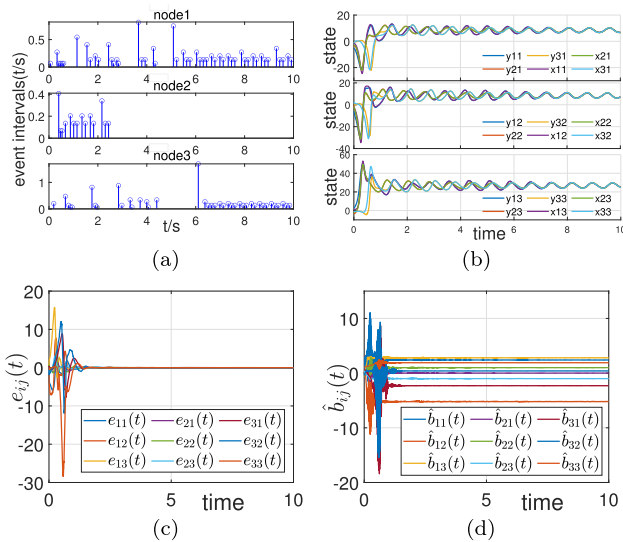


Fig. 11 Corollary 2 $\alpha = 0.7$: **a** The event intervals based on DETM (6); **b** The trajectories of $x_{ij}(t)$ and $y_{ij}(t)$; **c** The trajectories of $e_{ij}(t)$; **d** The trajectories of $\hat{b}_{ij}(t)$; $i, j = 1, 2, 3$

6 Conclusion

In this paper, we have discussed the topology identification and synchronization of FSPCNs in finite time via DETC. A topology observer and a DETM-based controller have been designed to derive the topology identification and synchronization in finite time. Moreover, it has been proved that Zeno behavior does not exhibit for the designed DETM.

In the future, it is a meaning endeavor to investigate the finite-time topology identification and synchronization of variable-order Fractional complex networks with discontinuous internal dynamics.

Author Contributions Lingyan Wang, Huaiqin Wu and Jinde Cao wrote the main manuscript text and Lingyan Wang prepared Figs. 1, 2, 3, 4, 5, 6, 7, 8, 9, 10 and 11. All authors reviewed the manuscript.

Declarations

Conflict of interest The authors declare that they have no conflict of interest.

Open Access This article is licensed under a Creative Commons Attribution 4.0 International License, which permits use, sharing, adaptation, distribution and reproduction in any medium or format, as long as you give appropriate credit to the original author(s) and the source, provide a link to the Creative Commons licence, and indicate if changes were made. The images or other third party material in this article are included in the article's Creative Commons licence, unless indicated otherwise in a credit line to the material. If material is not included in the article's Creative Commons licence and your intended use is not permitted by statutory regulation or exceeds the permitted use, you will need to obtain permission directly from the copyright holder. To view a copy of this licence, visit <http://creativecommons.org/licenses/by/4.0/>.

References

- Li M, Yu W, Zhang J (2023) Clustering analysis of multilayer complex network of Nanjing metro based on traffic line and passenger flow big data. *Sustainability* 15(12):9409
- Calabrese G, Molzahn C, Mayor T (2022) Protein interaction networks in neurodegenerative diseases: from physiological function to aggregation. *J Biol Chem.* <https://doi.org/10.1016/j.jbc.2022.102062>
- Saleh M, Esa Y, Mohamed A (2018) Applications of complex network analysis in electric power systems. *Energies* 11(6):1381
- Panda DK, Das S (2021) Smart grid architecture model for control, optimization and data analytics of future power networks with more renewable energy. *J Cleaner Prod* 301:126877
- Sakthivel R, Birundha Devi N, Harshavarthini S et al (2022) Disturbance estimation and synchronization control design for nonlinear complex dynamical networks with input delays. *Int J Robust Nonlinear Control* 32(7):4281–4299
- Pomerance A, Ott E, Girvan M, Losert W (2009) The effect of network topology on the stability of discrete state models of genetic control. *Proc Natl Acad Sci* 106(20):8209–8214
- Sakthivel R, Devi NB, Ma YK et al (2023) State estimation-based hybrid-triggered controller design for synchronization of repeated scalar nonlinear complex dynamical networks. *IEEE Access* 11:42069–42081
- Shahrampour S, Preciado V (2014) Topology identification of directed dynamical networks via power spectral analysis. *IEEE Trans Autom Control* 60(8):2260–2265
- Babakmehr M, Simoes M, Wakin M et al (2016) Smart-grid topology identification using sparse recovery. *IEEE Trans Ind Appl* 52(5):4375–4384
- Coutino M, Isufi E, Maehara T et al (2020) State-space network topology identification from partial observations. *IEEE Trans Signal Inform Process Netw* 6:211–225
- Zhu S, Zhou J, Chen G, Lu J (2019) A new method for topology identification of complex dynamical networks. *IEEE Trans Cybern* 51(4):2224–2231
- Zhao J, Aziz-Alaoui M, Bertelle C et al (2016) Sinusoidal disturbance induced topology identification of Hindmarsh-Rose neural networks. *Science China Inform Sci* 59(11):112205
- Liu H, Li Y, Li Z et al (2021) Topology identification of multilink complex dynamical networks via adaptive observers incorporating chaotic exosignals. *IEEE Trans Cybern* 52(7):6255–6268
- Tamil Thendral M, Ganesh Babu TR, Chandrasekar A et al (2022) Synchronization of Markovian jump neural networks for sampled data control systems with additive delay components: Analysis of image encryption technique. *Math Methods Appl Sci.* <https://doi.org/10.1002/mma.8774>
- Si G, Sun Z, Zhang H et al (2012) Parameter estimation and topology identification of uncertain fractional order complex networks. *Commun Nonlinear Sci Numer Simul* 17(12):5158–5171
- Li Z, Ma W, Ma N (2023) Partial topology identification of tempered fractional-order complex networks via synchronization method. *Math Method Appl Sci* 46(3):3066–3079

17. Rakkiyappan R, Chandrasekar A, Park JH et al (2014) Exponential synchronization criteria for Markovian jumping neural networks with time-varying delays and sampled-data control. *Nonlinear Anal Hybrid Syst* 14:16–37
18. Hai X, Yu Y (2020) Topology identification of fractional complex networks with an auxiliary network. *IFAC-PapersOnLine* 53(2):3675–3682
19. Bai J, Wu H, Cao J (2022) Secure synchronization and identification for fractional complex networks with multiple weight couplings under DoS attacks. *Comput Appl Math* 41(4):187
20. Diethelm K, Ford NJ (2002) Analysis of fractional differential equations. *J Math Anal Appl* 265(2):229–248
21. Kilbas A, Srivastava H, Trujillo J (2006) Theory and applications of fractional differential equations. Elsevier, Amsterdam
22. Jeong J, Lim Y, Parivallal A (2023) An asymmetric Lyapunov-Krasovskii functional approach for event-triggered consensus of multi-agent systems with deception attacks. *Appl Math Comput* 439:127584
23. Li Y, Song F, Liu J et al (2022) Decentralized event-triggered synchronization control for complex networks with nonperiodic DoS attacks. *Int J Robust Nonlinear Control* 32(3):1633–1653
24. Li H, Liao X, Chen G et al (2015) Event-triggered asynchronous intermittent communication strategy for synchronization in complex dynamical networks. *Neural Netw* 66:1–10
25. Bai J, Wu H, Cao J (2022) Topology identification for fractional complex networks with synchronization in finite time based on adaptive observers and event-triggered control. *Neurocomputing* 505:166–177
26. Zhang H, Gao Z, Wang Y et al (2021) Leader-following exponential consensus of fractional-order descriptor multiagent systems with distributed event-triggered strategy. *IEEE Trans Syst, Man, Cybern: Syst* 52(6):3967–3979
27. Hu W, Yang C, Huang T et al (2018) A distributed dynamic event-triggered control approach to consensus of linear multiagent systems with directed networks. *IEEE Trans Cybernet* 50(2):869–874
28. Du S, Liu T, Ho D (2018) Dynamic event-triggered control for leader-following consensus of multiagent systems. *IEEE Trans Syst, Man, Cybernet: Syst* 50(9):3243–3251
29. Li R, Wu H, Cao J (2022) Event-triggered synchronization in networks of variable-order fractional piecewise-smooth systems with short memory. *IEEE Trans Syst, Man, Cybern: Syst* 53(1):588–598
30. Wu Y, Shen B, Ahn CK et al (2021) Intermittent dynamic event-triggered control for synchronization of stochastic complex networks. *IEEE Trans Circuits Syst I Regul Pap* 68(6):2639–2650
31. Liu L, Zhou W, Li X et al (2019) Dynamic event-triggered approach for cluster synchronization of complex dynamical networks with switching via pinning control. *Neurocomputing* 340:32–41
32. Chai S, Lau V (2019) Joint rate and power optimization for multimedia streaming in wireless fading channels via parametric policy gradient. *IEEE Trans Signal Process* 67(17):4570–4581
33. Ren W, Jiang B, Yang H (2019) Singular perturbation-based fault-tolerant control of the air-breathing hypersonic vehicle. *IEEE-ASME Trans Mechatr* 24(6):2562–2571
34. Wang Y, Shi P, Yan H (2018) Reliable control of fuzzy singularly perturbed systems and its application to electronic circuits. *IEEE Trans Circuits Syst I Regul Pap* 65(10):3519–3528
35. Kokotović P, Khalil HK, O'reilly J. Singular perturbation methods in control: analysis and design. Society for Industrial and Applied Mathematics, pp 289–337 (1999). [https://doi.org/10.1016/0378-4754\(87\)90148-0](https://doi.org/10.1016/0378-4754(87)90148-0)
36. Cai C, Wang Z, Xu J et al (2014) An integrated approach to global synchronization and state estimation for nonlinear singularly perturbed complex networks. *IEEE Trans Cybernet* 45(8):1597–1609
37. Rakkiyappan R, Sivaranjani K (2016) Sampled-data synchronization and state estimation for nonlinear singularly perturbed complex networks with time-delays. *Nonlinear Dyn* 84:1623–1636
38. Zhang Y, Wu H, Cao J (2021) Global Mittag-Leffler consensus for fractional singularly perturbed multi-agent systems with discontinuous inherent dynamics via event-triggered control strategy. *J Franklin Instit Eng Appl Math* 358(3):2086–2114
39. Liang K, He W, Xu J et al (2021) Impulsive effects on synchronization of singularly perturbed complex networks with semi-markov jump topologies. *IEEE Trans Syst, Man, Cybern: Syst* 52(5):3163–3173
40. Hua T, Xiao J, Lei Y et al (2021) Dynamic event-triggered control for singularly perturbed systems. *Int J Robust Nonlinear Control* 31(13):6410–6421
41. Cheng J, Wang Y, Park J et al (2021) Static output feedback quantized control for fuzzy Markovian switching singularly perturbed systems with deception attacks. *IEEE Trans Fuzzy Syst* 30(4):1036–1047
42. Sivaranjani K, Rakkiyappan R, Cao J et al (2017) Synchronization of nonlinear singularly perturbed complex networks with uncertain inner coupling via event triggered control. *Appl Math Comput* 311:283–299
43. Shen H, Hu X, Wu X et al (2022) Generalized dissipative state estimation of singularly perturbed switched complex dynamic networks with persistent dwell-time mechanism. *IEEE Trans Syst, Man, Cybern: Syst* 52(3):1795–1806

44. Liang K, He W, Yuan Y et al (2022) Synchronization for singularity-perturbed complex networks via event-triggered impulsive control. *Discr Contin Dyn Syst-S* 15(11):3205–3221

Publisher's Note Springer Nature remains neutral with regard to jurisdictional claims in published maps and institutional affiliations.